



## INVESTIGATION OF NON-LINEAR CYCLES' PROPERTIES IN STRUCTURES SUBJECTED TO ENDURANCE TIME EXCITATION FUNCTIONS

M. Mashayekhi and H.E. Estekanchi<sup>\*,†</sup>

*Department of Sharif University of Technology, Tehran, Iran*

### ABSTRACT

Endurance Time Method (ET) is a dynamic analysis in which structures are subjected to intensifying accelerograms that are optimized in a way that seismic performance of structures can be estimated at different hazard levels with the best possible accuracy. For the currently available ET accelerograms, regardless of the shaking characteristic, an excitation level is recognized as a representative of a specific hazard level, when the acceleration and the displacement spectrum produced by the ET accelerograms up to that excitation level will be compatible with the acceleration and the displacement spectrum associated with that hazard level. This study compares the shaking characteristics of the current ET accelerograms with the ground motions. For this purpose, distribution of plastic cycles and the equivalent number of the cycles are considered as shaking properties of a motion. This study suggests a procedure to achieve the best possible consistency between the equivalent number of cycles of the current ET records and the ground motions. Moreover, a procedure to generate the new generation and optimization of the ET accelerograms which are more consistent with the ground motions are suggested.

Received: 17 December 2012; Accepted: 15 March 2013

**KEY WORDS:** equivalent hysteretic cycles; endurance time method; strong-motion duration; degrading materials; optimal dynamic analysis; performance based design

---

\* Corresponding author: H.E. Estekanchi, Sharif University of Technology, Tehran, Iran

†E-mail address: stkanchi@sharif.edu (H.E. Estekanchi)

## 1. INTRODUCTION

The peak amplitude of a ground motion is not a suitable predictor of structural performance because energy-dissipation capacity of the structure depends on the number of inelastic load cycles. In performance based design, it is assumed that a structure collapses when it is demanded to dissipate, through inelastic action, an amount of energy larger than supplied. In the performance-based design, in order to evaluate seismic motions, it is important to take the effect of the duration on the damage potential of the earthquake motion into account. Consequently, the demand of the dissipated energy which is highly dependent on shaking characteristics of earthquake motion should be predicted. In addition, it is experimentally demonstrated that there are many situation in which plastic cycles with low amplitude do not influence the damage; thus only a fraction of the plastic energy must be taken into account. The energy criterion consider all the plastic cycles in the same way by adding the dissipated energy of cycles independently regardless of those amplitudes. As a result of the limitation of the energy criterion, the effective number of cycles,  $n_{eq}$ , which consider the distribution of cycles is employed in this study. To sum up, the effective number of cycles represent shaking characteristics of an earthquake motion in a more realistic manner. Numerous authors tried to estimate seismic input energy in a structure [1-3].

The endurance time method is a dynamic analysis in which a structure is subjected to intensifying accelerograms and afterwards its performance is evaluated at the different hazard levels regarding the response of the structure at the certain excitation levels. These excitation functions are generated so that they have been matched to target spectrum (code spectrum or spectrum produced by the ground motions) whereas the duration consistency has not been directly considered. Production of optimal ET excitation functions that can produce better estimates of seismic response of structures is an open ended challenge in this respect. This study investigates the duration consistency of the current ET accelerograms with the ground motions considering the effective number of cycles as a reference parameter.

## 2. REFERENCE GROUND MOTION SET

Tendency to use the dynamic analysis for seismic assessment of structures is soaring among engineers. When the dynamic analysis is employed to analyze a structure, seismic motions used by this methodology can strongly influence the response of structures. Seismic motions can be represented by real, artificial, or even simulated records. Most seismic codes, such as ASCE standards 7-05 [4] relatively describe similar procedure for selection of seismic input motions.

The far-field record set for non-linear dynamic analysis which is proposed by FEMAP695 code is utilized in this study [5]. These motions can be applicable to structures located at different sites with different ground motion hazard functions, site and source conditions. A set of twenty two ground motions are used as listed in Table 1 which belong to bin of relatively large magnitudes of 6.5-7.6 proposed in FEMAp695 as far-field set.

Table 1. The suite of twenty two ground motion records used

ID No	Earthquake		Station
	M	Name	
1	6.7	Northridge	Beverly Hills-Mulhol
2	6.7	Northridge	Canyon Country-WLC
3	7.1	Ducze-Turkey	Bolu
4	7.1	Hector Mine	Hector
5	6.5	Imperial Valley	Delta
6	6.5	Imperial Valley	El Centro Array #11
7	6.9	Kobe, Japan	Nishi-Akashi
8	6.9	Kobe, Japan	Shin-Osaka
9	7.5	Kocaeli, Turkey	Ducze
10	7.5	Kcaeli, Turkey	Arcelik
11	7.3	Landres	Yermo Fire Station
12	7.3	Landres	Coolwater
13	6.9	Loma Prieta	Capitola
14	6.9	Loma Prieta	Gilory Array #3
15	7.4	Manjil, Iran	Abbar
16	6.5	Superstition Hills	Elcentro Imp. Co.
17	6.5	Superstition Hills	Poe Road (temp)
18	7.0	Cape Mendocino	Rip Del Overpass
19	7.6	Chi-Chi, Taiwan	CHY101
20	7.6	Chi-Chi, Taiwan	TCU045
21	6.6	San Fernando	LA-Hollywood Stor
22	6.5	Friuli, Italy	Tolmezzo

### 3. MAKE UP OF ET EXCITATION FUNCTIONS

The basic goal of ET analysis is to investigate the performance of structures in different hazard levels by using only one time history analysis. The ET analysis uses intensifying accelerograms which response of structures at different times can be used to evaluate the performance of structures at corresponding hazard level. Each time, the ET analysis can be interpreted as a representative of specified hazard level. For instance, if time window of 10 seconds produces DBE hazard level acceleration spectrum in one ET accelerogram, the response of structure at 10 seconds is the representative of DBE performance level. It means that if drift ratio of structure at 10 seconds does not exceed the acceptable drift criteria at LS performance level, the structure satisfies the LS performance level at DBE hazard level. One intensifying ET accelerogram is depicted in Figure 1.

Intensifying accelerograms used in the ET analysis are generated so that they make meaningful correspondence between the response of a structure at a particular time in the ET analysis and the average of response to ground motions at specified hazard level. These ground motions should reflect the hazard level at certain site. The response of a structure due to an ET accelerogram increases by time; hence at each time window, this acceleration

function can be attributed to a particular hazard level regarding the acceleration spectrum produced by the ET accelerogram. In spite of the fact that each excitation level of the ET records can be representative of the specified hazard level, the current ET records are matched only at one hazard level (i.e. DBE hazard level) at a particular time called target time. In the current ET records, for other times, the produced spectrum by the ET excitation functions varies linearly as:

$$S_{ac}(T, t) = \frac{t}{t_{target}} S_{ac}(T) \quad (1)$$

where  $S_{ac}(T)$  is the target spectrum,  $S_{ac}(T, t)$  is the spectrum to be produced at time  $t$  by the ET excitation functions, and  $t_{target}$  stands for target time.

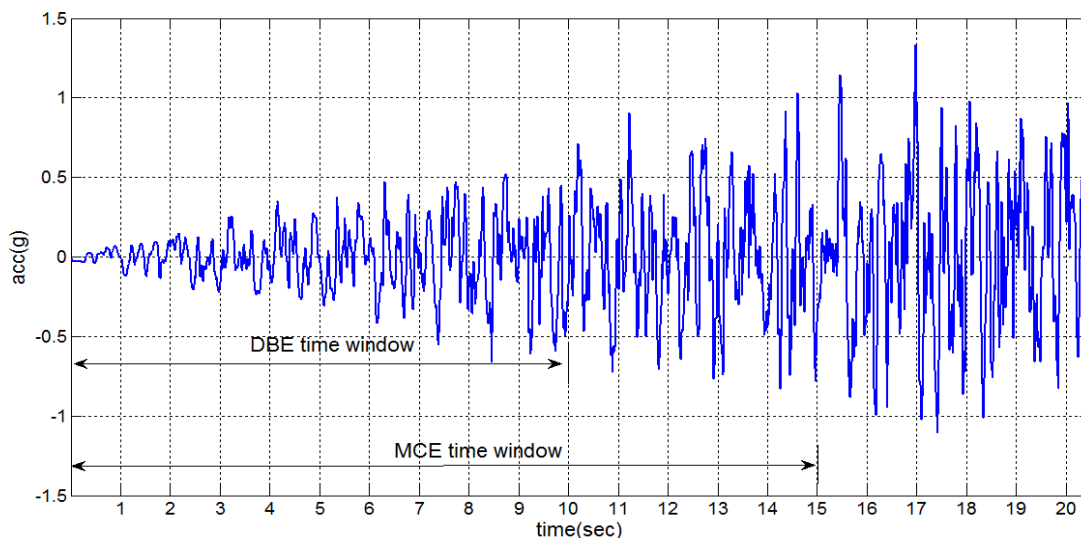


Figure 1. ETA20e01 acceleration function

Displacement spectrum is also highly important consideration to characterize a dynamic excitation. Target displacement spectrum can be defined as a function of acceleration spectrum as [6]:

$$S_{uc}(T, t) = \frac{t}{t_{target}} S_{ac}(T) \times \frac{T^2}{4\pi^2} \quad (2)$$

where,  $S_{uc}(T, t)$  is the target displacement spectrum to be induced at time ( $t$ ) by the ET excitation functions.

Given the Eqs 1 and 2, it is shown that ET accelerograms should produce template

acceleration spectrum at a specified time called target time and produce proportion of template acceleration spectrum at other times which this proportion is linear fraction of length of time window to the target time. For the current ET accelerograms, the target time equals to 10 seconds as a criteria to be used in previous research which was only an engineering judgment. ETA20e series of ET accelerograms consist of three acceleration functions, namely ETA20e01, ETA20e02, and ETA20e03 which average acceleration spectra of a set of seven ground motions is its template acceleration spectrum. Nonlinear optimization is used to generate this series of ET accelerograms. The acceleration spectrum of this series of ET accelerograms at target time (10 second), 5second, and 10 second is depicted in Figure 2 as below:

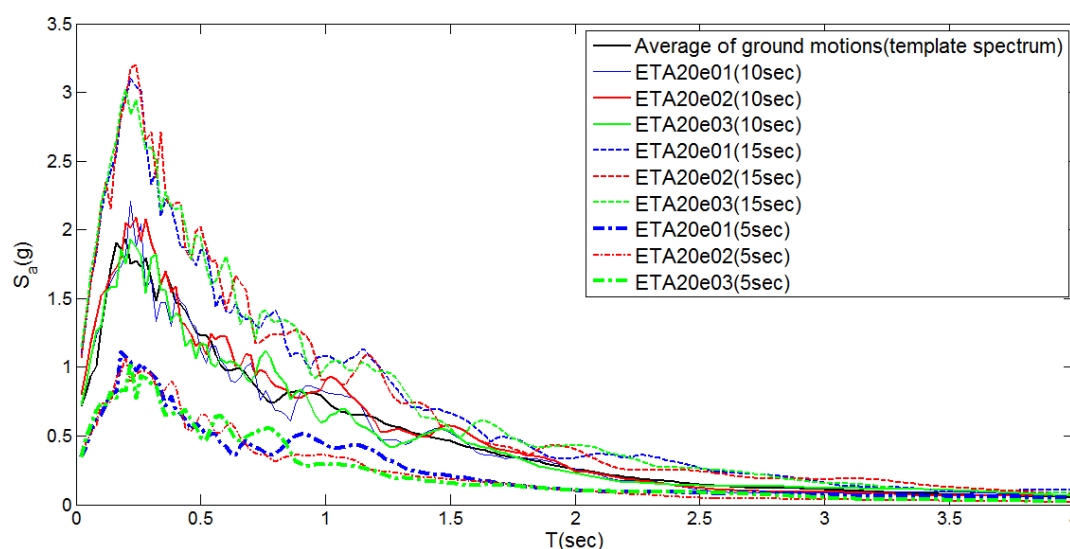


Figure 2. Acceleration spectra of ET accelerograms at different time window

In the second generation of ET excitation functions, the concept of response spectrum and numerical optimization are introduced and numerically significant results are achieved [7]. By extending the range of period of vibration into very long periods, the records in this generation also produce highly reasonable estimates in non-linear range of behavior [8]. In the third generation, non-linear response spectra are included in the optimization procedure [9]. Recently, some researchers use these ET excitations in their works. For instance, Avanaki and Estekanchi investigated the collapse analysis by ET method [10]. This study uses ETA20e series of ET excitation function and suggests suitable target time at which in addition to intensity and frequency content, shaking characteristic of the ground motions is considered.

#### 4. DEFINITIONS OF EQUIVALENT NUMBER OF CYCLES

Some authors consider the input energy, i.e. hereafter  $E_I$ , as an effective tool in the seismic

design stating that  $E_I$  represents a highly usable parameter of the structural response and it hardly depends on the hysteretic properties of the structure [1-3]. However, it is necessary to observe that a part of input energy transmitted to structure is dissipated by means of the damping, while another is dissipated by means of the hysteretic energy. It should be noted that only the amount of dissipated energy due to the inelastic deformation is considered to induce damage into structure. Unlike the input energy, the amount of hysteretic energy dissipated by the structure depends on the properties of the structure including the period and strength of the structure and its ductility ratio.

It is possible to define damage criteria based on the assumption that the structural collapse occurs when the hysteretic energy dissipated under seismic motion is equal to the energy dissipated under monotonic load. The allowable hysteretic energy can be evaluated by the means of theoretical and experimental analysis of monotonic tests. The seismic check is represented by the relation as:

$$E_h < E_{h,u} \quad (3)$$

where  $E_{h,u}$  represents the allowable hysteretic energy of the analyzed structure.

However, the energy criterion has the limitation to consider all plastic cycles in the same way adding the dissipated energy regardless of the amplitude of each cycle. A measure which considers the distribution of cycles with different amplitude is the equivalent number of cycles  $n_{eq}$  [1]. This parameter represents the number of cycles at the maximum displacement which the structure can develop in order to dissipate the total amount of the hysteretic energy  $E_H$ :

$$n_{eq} = \frac{E_H}{F_y (x_{max} - x_y)} \quad (4)$$

where  $E_H$  is the total dissipated energy,  $F_y$  as the strength of structure,  $x_{max}$  as the maximum displacement and  $x_y$  as the displacement at elastic limit.

The  $n_{eq}$  varies from values close to 1 for impulsive earthquakes with strong pulse to the values of about 30-40 for long-duration earthquakes [1]. Values of  $n_{eq}$  close to 1 show the presence of a large plastic cycle in the nonlinear response; while high values of  $n_{eq}$  are indicative of the presence of many plastic cycles with different amplitudes [1].

In this study, the equivalent number of cycles is defined as the number of cycles with the maximum hysteretic energy which is required to dissipate the total hysteretic energy. This parameter is more useful than the equivalent number of cycle definition used by other authors to predict the distribution of plastic cycles of a motion. The most useful property of this definition is its capability to apply to the material with degrading and deterioration behavior. This definition is illustrated in Figure 3:

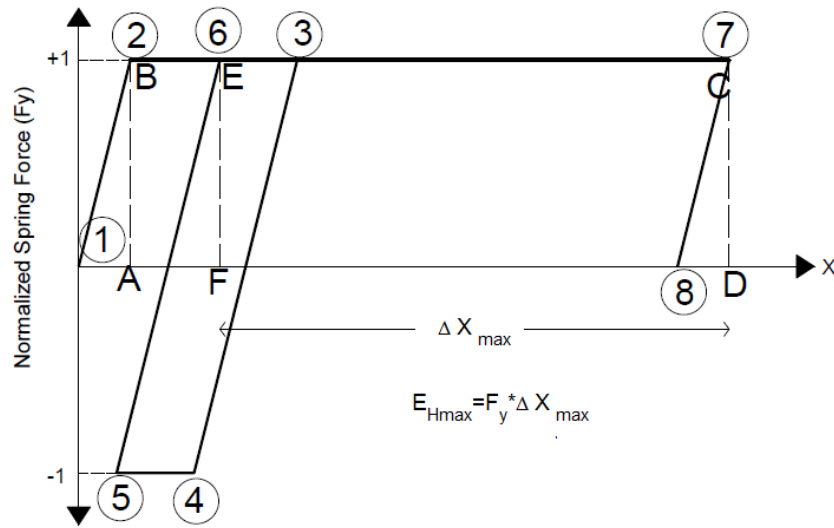


Figure 3. Illustration of the equivalent number of cycles

$$n_{eq} = \frac{E_H}{E_{hmax}} \quad (5)$$

In this paper, the equivalent number of cycles is defined as the number of cycles with  $E_{hmax}$  which is required to dissipate the total hysteretic energy ( $E_H$ ); whereas several authors define the equivalent number of cycles as the number of cycles with the maximum displacement which is required to dissipate the total hysteretic energy. A structure under severe earthquake dissipate part of input energy through number of nonlinear cycles which each of them dissipate part of the total hysteretic energy; whereas all these cycles contribute damage into structure. However, the cycle with the maximum dissipated energy have the highest contribution damage into structure and hence is higher under consideration.  $E_{hmax}$  is the maximum dissipated energy in one cycle; for instance, the area of the rectangular CDFE in Figure 3 and cycles with the maximum displacement are the cycles with hysteretic energy equals to the  $F_y(x_{max}-x_{min})$  For instance, the area of the rectangular ABCD in Figure 3.

Necessarily, there is no inelastic cycle in which the dissipated energy is equal to  $F_y(x_{max}-x_{min})$  in a motion and hence, the  $n_{eq}$  which is calculated by using the Eq. 2 is not perfectly appropriate to observe the distribution of inelastic load cycles in the motion.

In addition, cyclic ductility ratio,  $\mu_c$  is employed in order to quantify the extent of the nonlinear behavior in the structure. This quantity is defined as below:

$$\mu_c = 1 + \frac{\Delta x_{max}}{x_y} \quad (6)$$

For a symmetric motion, cyclic ductility ratio is equal to twice of the ductility ratio,  $\mu$  as:

$$\mu = \frac{x_{\max}}{x_y} \quad (7)$$

Herein, a structure is modeled as mass-spring-dash pot which its spring exhibits nonlinear behavior during severe earthquake. This structure is subjected to Northridge (1944)/Beverly Hills- Mulhol; afterwards the force-deformation is demonstrated in Figure 4(a). It should be mentioned that the rule for nonlinear spring is compiled by Ibarakrawilinker material model [11] and the strength level of structure is 0.046 mg. The basic rule for this hysteretic model is shown in Figure 5. Moreover, the distributions of plastic cycles are depicted in Figure 4(b) as below.

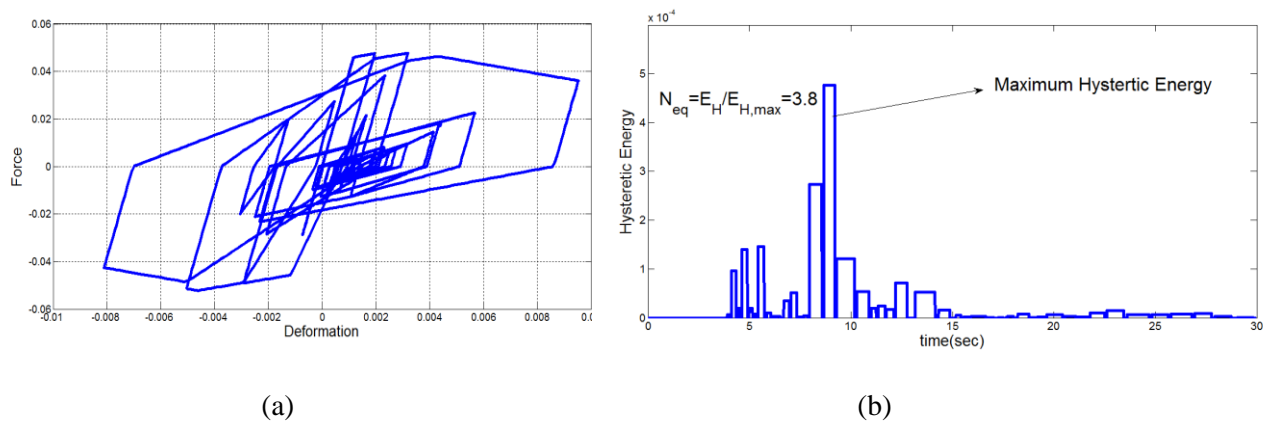


Figure 4. (a) The force-deformation behavior of nonlinear spring (Northridge (1944)/Beverly Hills- Mulhol); (b) Distributions of plastic cycles in nonlinear spring (Northridge (1944)/Beverly Hills- Mulhol)

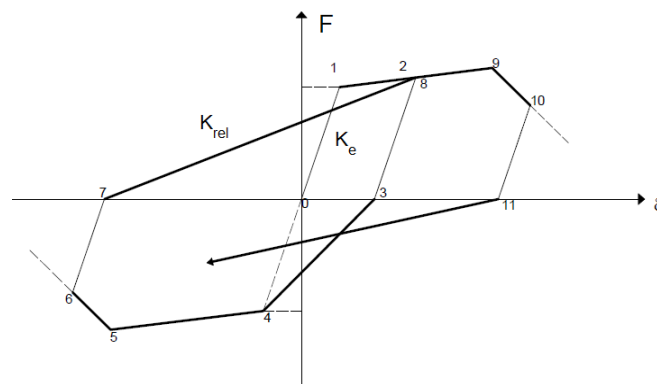


Figure 5. Peak oriented hysteretic model

The number of nonlinear cycles is estimated (3.8) by using the proposed formula; whereas if Eq. 2 is adopted, number of nonlinear cycles is derived (4.7). It is observable that



4.7 is not accurate estimation of the number of nonlinear cycles in the motion which is illustrated in fig 4.b. The strongest reason is arisen from the fact that Eq. 2 is not for degrading material.

### 5. A COMPARISON BETWEEN EQUIVALENT NUMBER OF CYCLES OF THE GROUND MOTIONS AND ET RECORDS

In this part, the equivalent number of cycles for both the ground motions and the ET records are computed. The equivalent number of cycles is computed for the records at a specified cyclic ductility ratio (in this study at  $\mu_c=2, 4, 6$ ). Figure 6 shows the  $n_{eq}$  for the ground motions at cyclic ductility ratio which equals to 6. The dispersion of the  $n_{eq}$  for ground motions is significant; whereas they have identical cyclic ductility ratio.

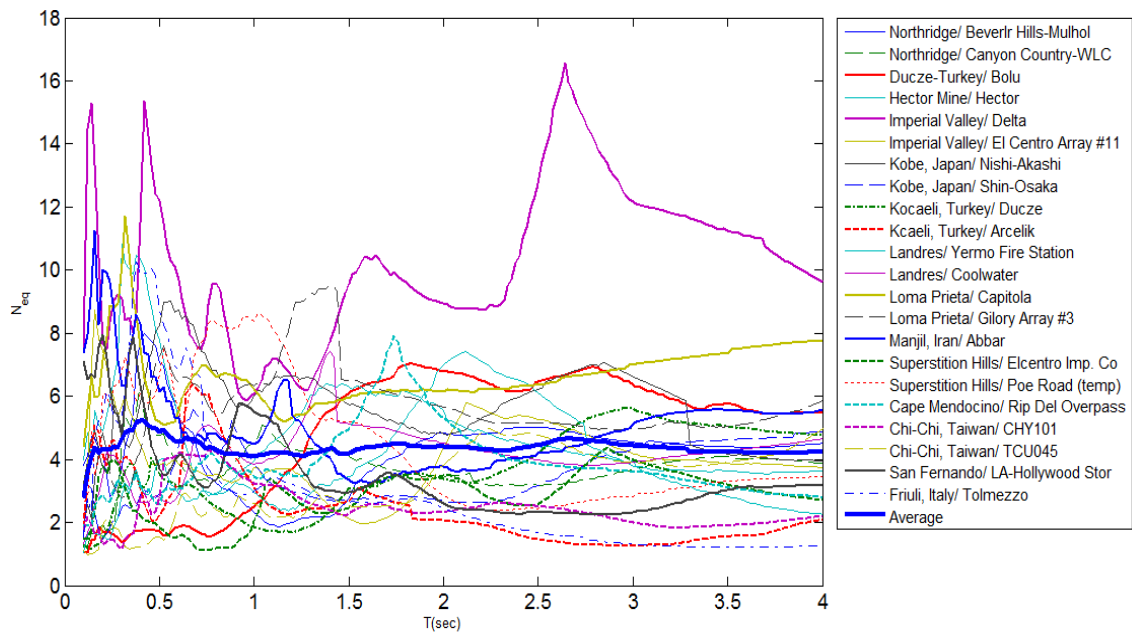


Figure 6. The equivalent number of cycles for the ground motions at  $\mu_c=6$

Dispersion of number of cycles of different ground motions implies that equality of cyclic ductility and hence severity of nonlinearity of structure subjected to different ground motions cannot guaranty the equality of number of cycles. In addition, Figure 7 compares the  $n_{eq}$  of the average of the ground motions at different ductility ratio.

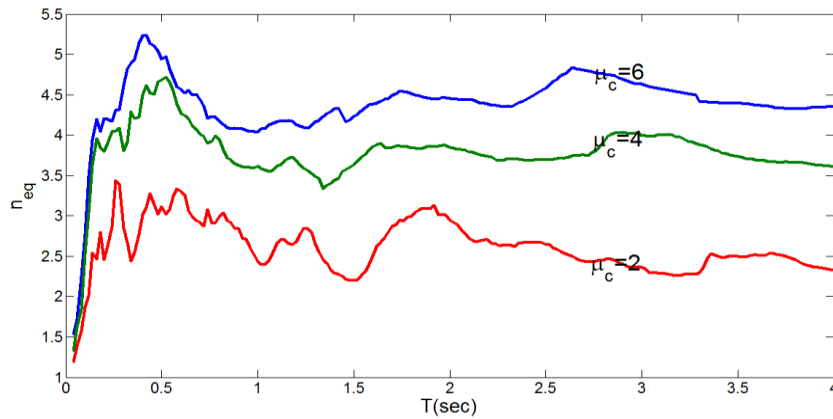


Figure 7. Influence of cyclic ductility ratio on  $n_{eq}$  in ground motions

Figure 7 shows that the trend of variation of the  $n_{eq}$  is approximately similar for different target cyclic ductility. The equivalent number of cycles of a motion,  $n_{eq}$ , generally increase up to about the characteristic period ( $T_c$ ) and remain nearly constant for the period range after characteristic period [7]. The characteristic period is defined as:

$$T_c = 2\pi \frac{c_v \ddot{x}_{g \max}}{c_a \dot{x}_{g \max}} \quad (8)$$

where  $c_a$  is the ratio of elastic spectral acceleration to peak ground acceleration in the short period range and  $c_v$  is the ratio of the spectral velocity to the peak ground velocity in the velocity-controlled range of response and  $\ddot{x}_{g \max}$  and  $\dot{x}_{g \max}$  is the peak ground acceleration and peak ground velocity, respectively.

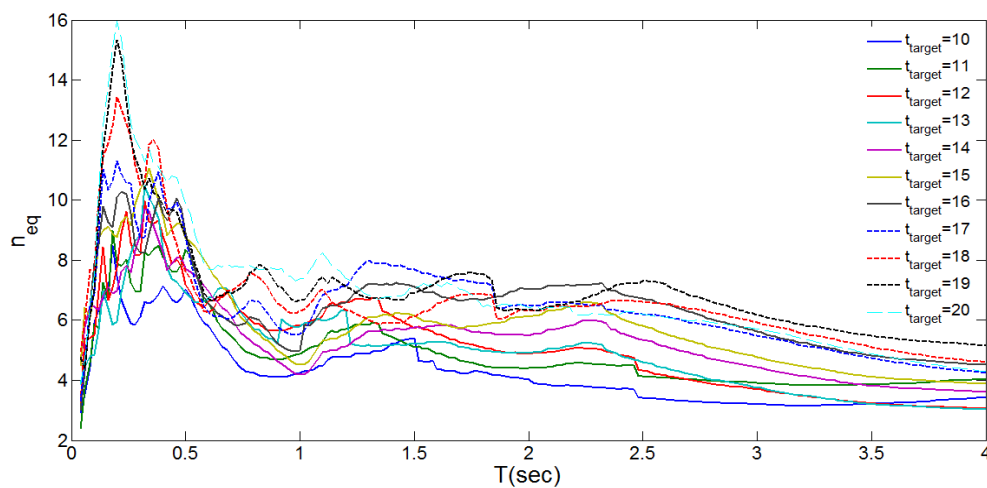


Figure 8. Influence of target time on the  $n_{eq}$  in ETA20e for  $\mu_c=6$

The  $n_{eq}$  of an ET accelerogram depends on the target time at which they are scaled. Figure 8 shows the differences between the  $n_{eq}$  of ETA20e series when the target time is altered.

It can be mentioned that the  $n_{eq}$  generally increases with increasing the target time. Therefore, it should be considered to determine target time which makes the best correspondence between the shaking characteristics of the ET records and the ground motions.

In addition, the target time in which the ground motions and ET records are highly duration consistent should be determined. In order to answer this question, Figure 9 is plotted to compare the  $n_{eq}$  of the ET records with  $n_{eq}$  of the ground motions at certain cyclic target ductility ratios.

Excitation functions and the ground motions Figure 9 shows that target time for periods lower than 1second is less than 10 seconds and for periods higher than 1 second is greater than 10 seconds. This issue emphasizes the fact that target times for different periods are different; hence, target times should be determined separately for each single period. For period of 1 second and cyclic ductility equaling to 6, variation of number of cycles of ET records versus time is demonstrated in Figure 10 and schematically the number of cycles of ET excitation functions is compared with the average ground motions.

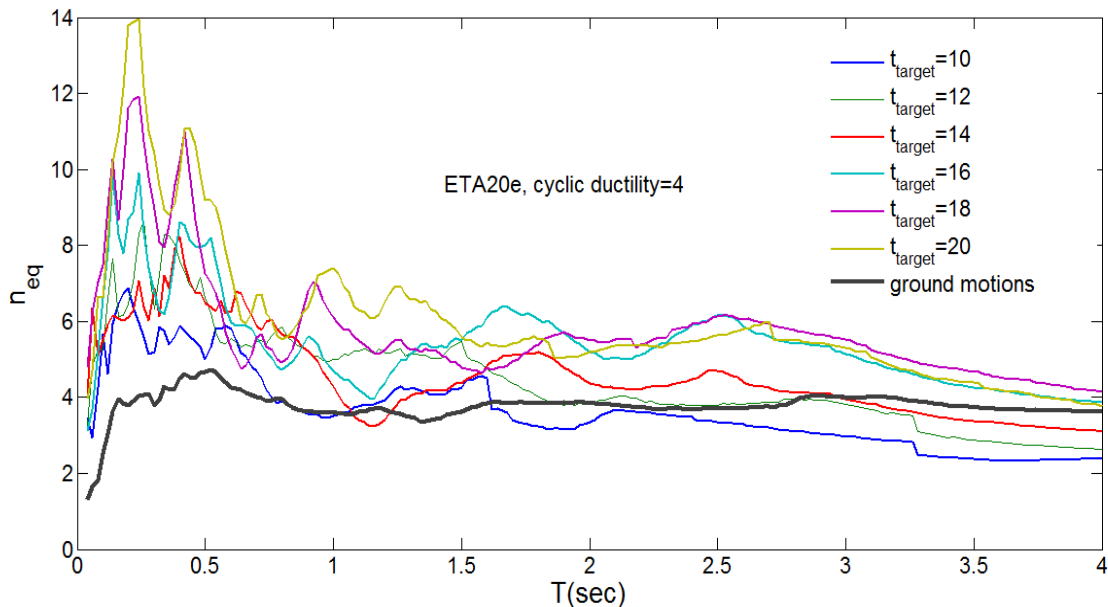


Figure 9. Comparison between the equivalent number of cycles of the ETA20e01-03

In Figure 10, variation of number of cycles of ET records is approximated by linear function of time. In Figure 11, the variation of number of cycles of ET records for three different periods are depicted and compared. It should be mentioned that the lines in Figure 10 is linear representative of the actual variation of number of nonlinear cycles similarly to the one used in Figure 9.

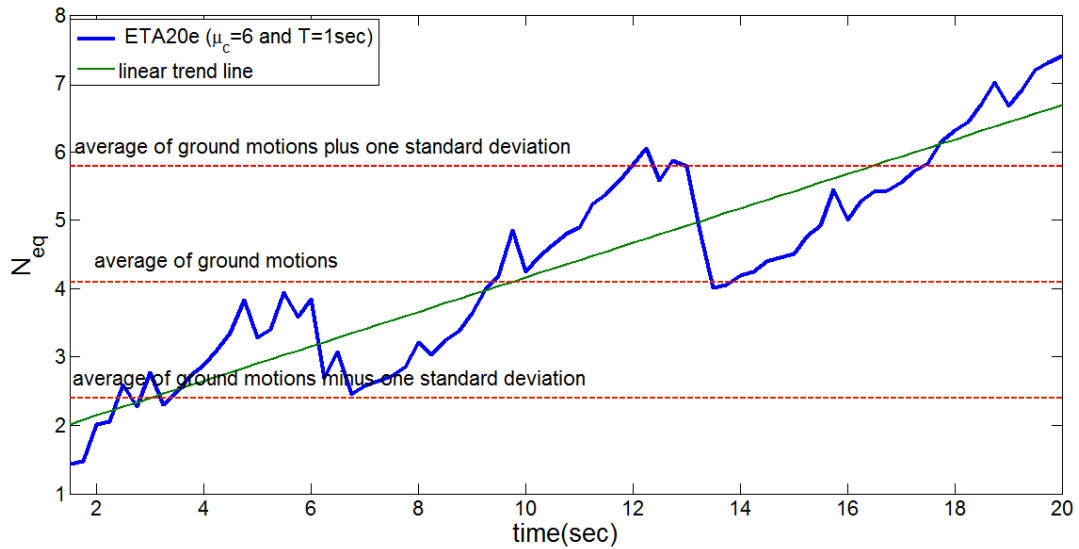


Figure 10. Comparison of number of cycles of ETA20e with ground motions

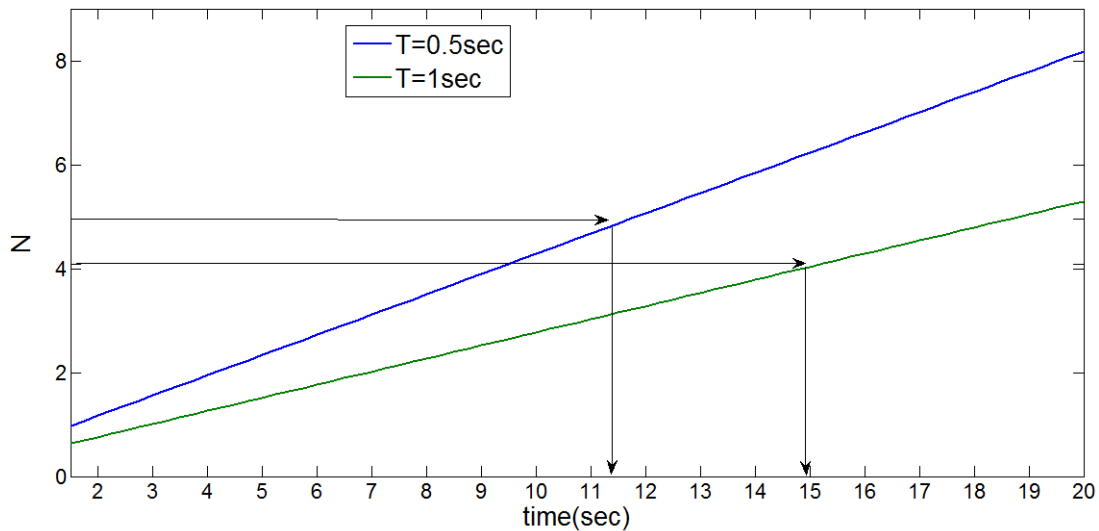


Figure 11. Comparison of variation of number of cycles of ETA20e records for three different periods

Figure 11 shows that the ET records make stiffer structures to endure more number of cycles; moreover, slope of variation of number of cycles for low periods is steeper than high periods. Figure 12 illustrates the target time versus period which is derived similarly to procedure shown in Figure 10 for different cyclic ductility. These target times are calculated based on the fact that the structure subjected to the ET records experience the number of cycles equal to the average number of cycles when that structure is subjected to ground motions. These target times are associated with different structures with certain linear

period and a specified cyclic ductility.

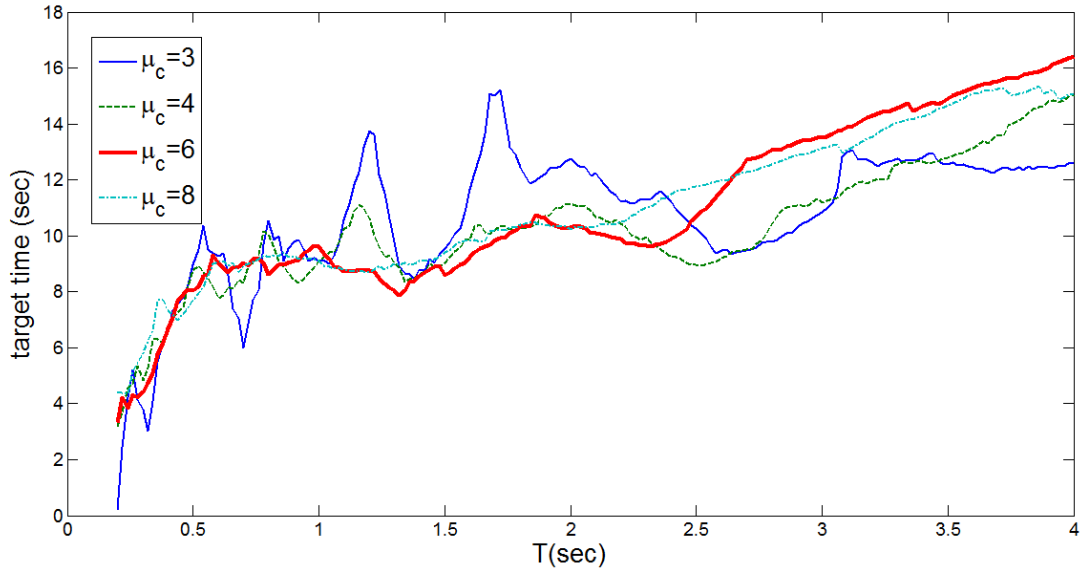


Figure 12. Target times versus period for different values of cyclic ductility (ETA20e series)

Target times for cyclic ductility equal to 4, 6, and 8 roughly have subtle dispersion. In Figure 13, correlation factor of variation of  $n_{eq}$  (number of nonlinear cycles) against time for different cyclic ductility is presented. This is due to the fact that to investigate the accuracy of target times is computed based on assumption of linear variation.

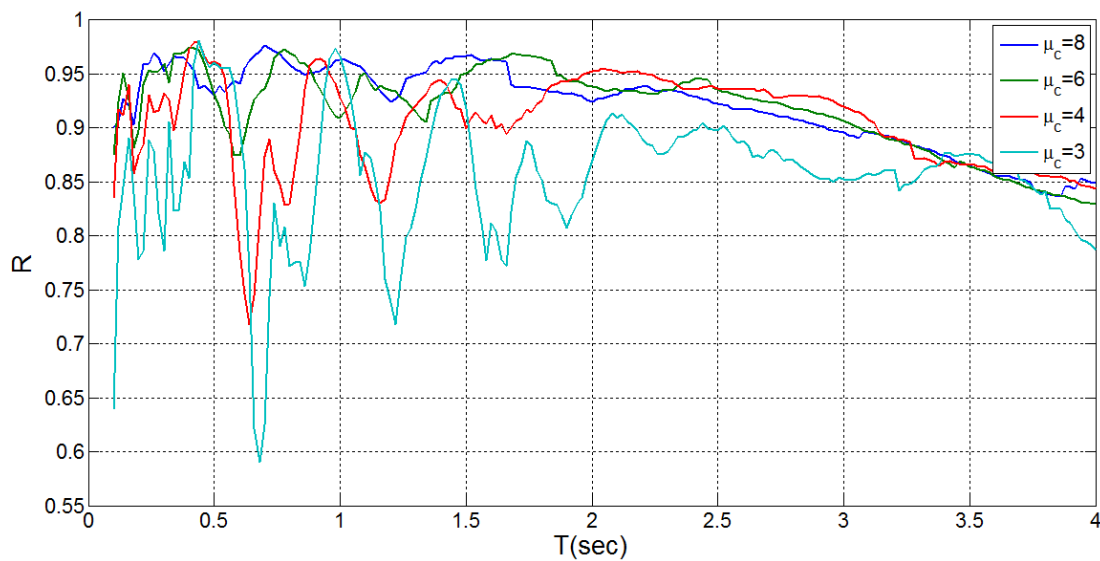


Figure 13. Correlation factor of variation of number of cycles against time for different cyclic ductility

It is shown that for cyclic ductility equal to 4, 6, and 8, the correlation factor is significantly high and even close to 0.95.

In order to consider the margin of safety and the dispersion of number of cycles of ground motions, another group of target times are proposed so that the ET records at those target times, produce the number of cycles equal to the average plus one standard deviation number of cycles of ground motions. The results are presented in Figure 14 for cyclic ductility equal to 6, and 8 because in these two values of cyclic ductility, the correlation factor are reliably high and appropriate for the sake of preciseness as previously shown in Figure 13.

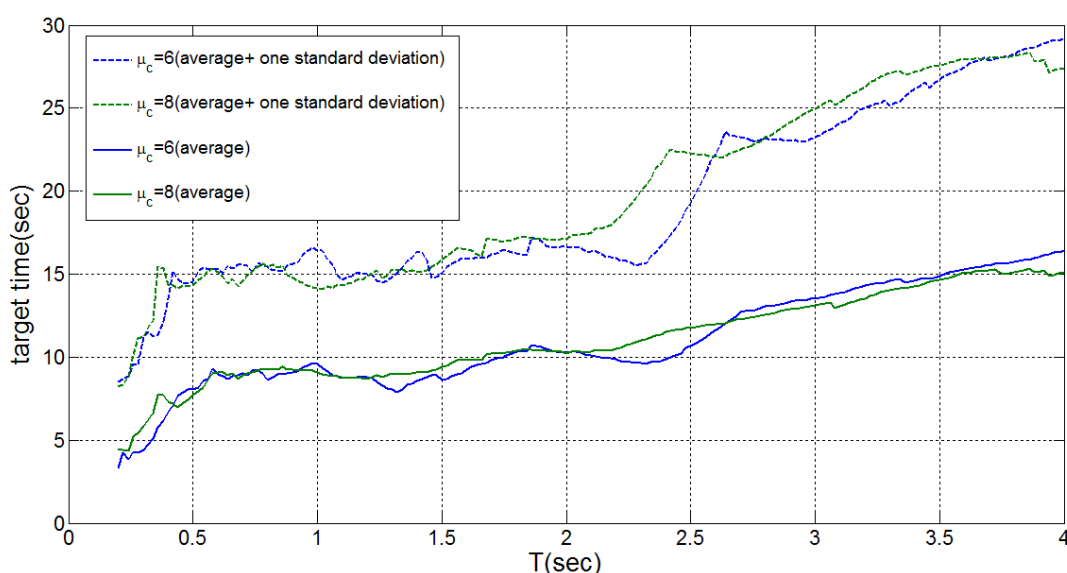


Figure 14. Target times for average and average plus one standard deviation for ETA20e

For the sake of simplicity, 15 seconds can be chosen as constant target time for all periods and obviously this value of target time guaranties the fact that the ET records make the structures to dissipate hysteretic energy through number of cycles. This value is consistent with number of cycles associated with ground motions.

## 6. EXAMPLE FOR A SDOF SYSTEM

A SDOF structure with linear period of 3 sec. with degrading behavior is subjected to both the ground motions and the ET records. The strength level of this structure is 0.0625 fraction of its weight. In this analysis, the reference acceleration spectrum is INBC (Iranian National Building Code) code design [13]. For the case of ET records, three target times including 5 sec, 8 sec, and 15 sec. are adopted. It should be noted that response parameters have been extracted through the moving average of responses as shown in Figure 15. Two response parameters are employed in this study including ductility demand and Park-Ang

damage index which are presented in Eq.s 9 and 10, respectively. In Park-Ang damage index, damage is expressed as linear combination of the maximum deformation and the effect of repeated cyclic loading [12].

$$\mu = \frac{x_{max}}{x_y} \tag{9}$$

$$DI_{park-Ang} = \frac{x_{max} - x_y}{x_{mon} - x_y} + \beta \frac{E_H}{F_y x_y} \tag{10}$$

which  $x_{max}$ ,  $x_y$ ,  $x_{mon}$ ,  $E_H$ ,  $F_y$ ,  $\beta$  are the maximum displacement under earthquake loading, yield displacement, the maximum displacement under monotonically increasing displacement loading, hysteretic energy, strength level of structure and non-dimension coefficient, respectively.

The maximum responses are plotted versus time in Figure 15. This curve is not used directly to predict responses; on the other hand, the moving average of this curve is computed. Moreover, based on the moving average of responses, the structural performance is evaluated in the ET analysis. This approach is employed in order to remove the influence of randomness data from the output result of ET analysis. Three ET curve based on three different target times are plotted in Figure 15. Differences in these curves are arisen from the fact that in these curves, the time in which ET accelerograms produce acceleration spectrum of code is different. For example, if target time is 5 seconds, ET accelerograms produce acceleration spectrum of the code design at time window equal to 5 seconds and hence, the response of structure should be read at this time from moving average of the ET curve.

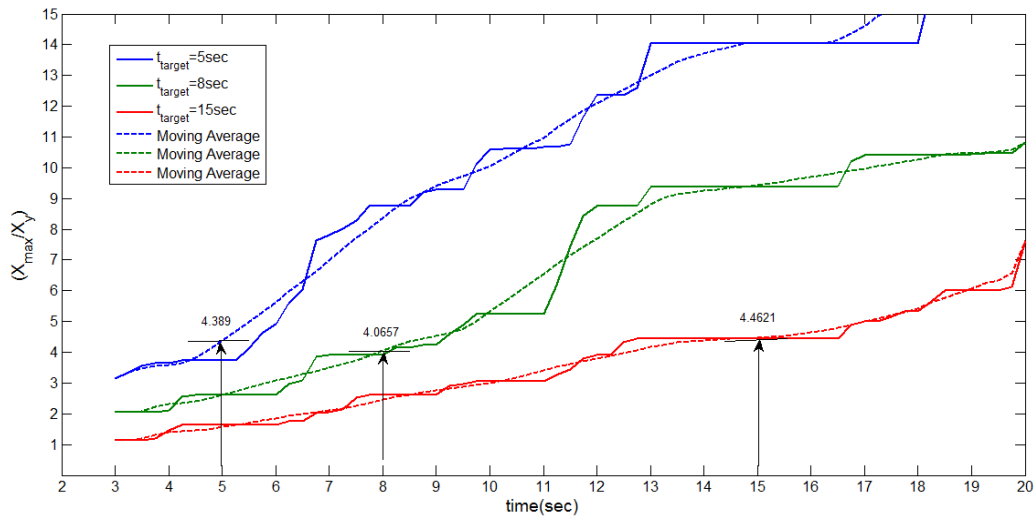


Figure 15. Response parameter of structure subjected to ET records ( ET curve)

For quantification of the effectiveness of the each target times, quantities of *errd* and *errp* are defined in Eqs 11, 12 as below:

$$errd(\%) = \frac{\mu(ETrecords) - \mu(average\ motions)}{\mu(average\ motions)} \quad (11)$$

$$errp(\%) = \frac{DI_{P-A}(ETrecords) - DI_{P-A}(average\ motions)}{DI_{P-A}(average\ motions)} \quad (12)$$

The results of analysis are summarized in Table 2 as below:

Table 2. Error percentage for the ET analysis of the structure

	Target =5sec	Target=8sec	Target=15sec
<i>errd</i>	0.19%	-7.18%	1.86%
<i>errp</i>	-22.2%	-26.68%	-11.12%

Hysteretic curve of the SDOF structure when structure is subjected to ETA20e01 with target time equals to 5second, 8second, and 10second, respectively as depicted in Figure 16 below:

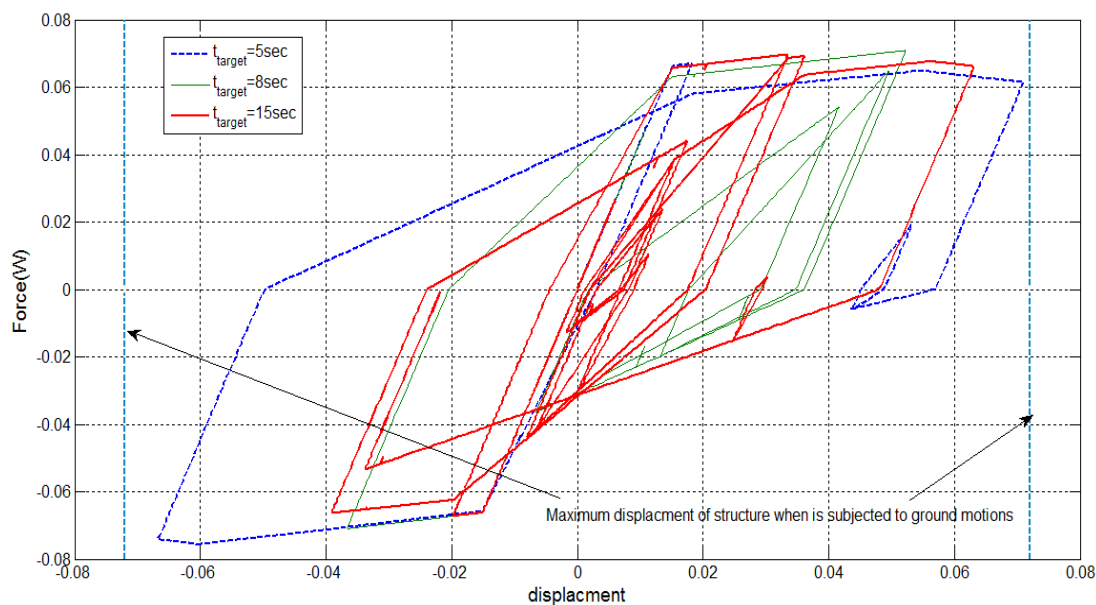


Figure 16. Hysteretic curve of structure when it is subjected to ETA20e01 with different target time

It is shown in Figure 16 that when target time is 5 seconds or 8 seconds, the structure



does not experience sufficient number of cycles; hence, it does not encounter the degrading and deterioration behavior which may dramatically influence the responses and the predicted performance of structure. This inconsideration of degrading and deterioration behavior of structure as well as hysteretic energy which might be underestimated as a result of low number of cycles, can make appreciable error in results. Therefore, target time equaling to 15 seconds can reasonably predict response of the structure as a consequence of more consistency of number of cycles with ground motions compared to other target time.

Table 2 presents that target time equal to 5 seconds precisely predict the average displacement of the structure when it is subjected to ground motions; however, the structure in this manner does not experience sufficient number of cycles. Since the structure does not encounter the degrading and deterioration behavior and also does not dissipate adequate hysteretic energy, Park-Ang damage index is not accurately predicted by the ET analysis using this target time.

It can be concluded that Park-Ang damage index is more sensitive to number of cycles; hence, it is well predicted when the ET records make the structure dissipate hysteretic energy through number of cycles which is more consistent with ground motions.

## 7. CONCLUSION

The following conclusions can be drawn based on the result of this research:

1) The number of nonlinear cycles of a motion increases with an increase in the target cyclic ductility. It means that when the structure exhibits more nonlinear behavior, the structure dissipates hysteretic energy through more number of nonlinear cycles. The number of nonlinear cycles of the ET records depends on their target time so that the ET records with longer target time have more equivalent number of cycles compared to the others.

2) The numbers of nonlinear cycles of the current ET records are compared with the number of nonlinear cycles of the ground motions. The target time is determined in each single period to ensure that when structure is subjected to both the ET records and ground motions, it experiences roughly identical number of cycles. Therefore, the considered target time should be a function of the main period of structure as well as its nonlinear characteristic such as cyclic ductility where it is used in this study.

3) Since dispersion of number of nonlinear cycles of ground motions is appreciably high and record-to-record variability of this quantity is considerable, to determine the target time barely based on average of ground motions is not useful; hence, target time should be determined not only based on the average but also the standard deviation of number of cycles of ground motions. In this study, the target time is proposed in two general viewpoints; first, based on the average of ground motions and second, based on the average plus one standard deviation.

4) For the sake of simplicity, 15 seconds can be chosen as constant target time for all periods and obviously, this value of target time guaranties the fact that the ET records make the structures dissipate hysteretic energy through number of cycles which is consistent with the number of cycles associated with ground motions. Those damage indices which depend on the hysteretic energy and cyclic characteristic of materials are more susceptible to

duration and number of nonlinear cycles of motions compared to those damage indices that only are dependent on the maximum deformation or displacement.

5) By analyzing a SDOF structure, the effectiveness of proposed target time is investigated. It is shown that when a low value of target time is chosen in the ET analysis, the structure does not experience several cycles and generally dissipates its whole hysteretic energy in approximately one cycle. Consequently, the structure does not encounter degrading and deterioration behavior which might deal with when it is subjected to ground motions.

6) For realistic evaluation of structural performance, hysteretic energy and repeated cycle should be considered in an analysis. This study emphasizes that the target time should be under consideration for the ET analysis to predict Park-Ang damage index. This study also suggests the new cycle counting definition to be used for optimization and generation of the next generation of ET accelerograms which will be more duration consistent with ground motions than currently available ET accelerograms.

#### Acknowledgement:

The authors would like to thank Sharif University of Technology Research Council for their support of this research.

#### Nomenclature:

$c_a$	Ratio of elastic spectral acceleration to peak ground acceleration in the short period range
$c_v$	Ratio of the spectral velocity to the peak ground velocity in the velocity-controlled range of response
$DI_{Park-Ang}$	Park-Ang damage index
$E_H$	Hysteretic energy
$E_{H\max}$	Maximum hysteretic energy
$E_{mon}$	Allowable hysteretic energy of the analyzed structure
errd	Percentage of displacement error
errp	Percentage of Park-Ang damage index error
$F_y$	Strength of structure
g	Acceleration due to the gravity
$S_{aC}(T)$	Target spectrum
$n_{eq}$	Equivalent number of cycles
$S_{aC}(t, T)$	Acceleration spectrum to be induced at time t
$S_{uC}(t, T)$	Target displacement spectrum at time t
T	Free Vibration Period

$t$	Time
$x_{\max}$	Maximum displacement
$x_y$	Yield displacement
$\ddot{x}_{g \max}$	Peak ground acceleration
$\dot{x}_{g \max}$	Peak ground velocity
$\beta$	Non-dimension coefficient
$\Delta x_{\max}$	Maximum cyclic displacement
$\mu_c$	Cyclic ductility
$\mu$	Ductility

### REFERENCES

1. Manferdi G. evaluation of seismic energy demand, *Earth. Eng Struct Dyn*, 2001; **30**: 485–99.
2. Uang CM, Bertero VV. Evaluation of seismic energy in structures, *Earthq Eng Struct Dyn*, 1990; **19**: 77–90.
3. Fajfar P, Vidic T. Consistent inelastic design spectra: hysteretic and input energy, *Earthq Eng Struct Dyn*, 1994; **23**: 523–38.
4. ASCE. *Minimum design load for building and other structures ASCE Standard No. 007-05*, American society of civil engineers, Virginia, USA, 2005.
5. FEMA. *Quantification of Building Seismic performance Factors, FEMA695*, Federal Emergency Management Agency, Washington DC, USA, 2009.
6. Estekanchi HE, Valamanesh V, Vafai A. Application of endurance time method in linear seismic analysis, *Eng Struct*, 2007; **29**(10): 2551–62.
7. Valamanesh V, Estekanchi HE. Characteristics of second generation endurance time method accelerograms, *Scientia Iranica*, 2010; **17**(1): 53–61.
8. Riahi HT, Estekanchi HE. seismic assessment of steel frames with endurance time method, *J Construct Steel Res*, 2010; **66**(6): 780–92.
9. Nozari A, Estekanchi HE. Optimization of Endurance Time acceleration functions for seismic assessment of structures, *Int J Optim Civi. Eng*, 2011; **2**: 257–77.
10. Avanaki MJ, Estekanchi, HE. Collapse analysis by Endurance Time method, *Int J Optim Civi. Eng*, 2012; **2**(2): 287–99.
11. Ibarra LF, Medina RA, Krawinkler H. Hysteretic models that incorporate strength and stiffness deterioration, *Earthq Eng Struct Dyn*, 2005; **34**: 1489–511.
12. Park YJ, Ang AH. Mechanistic seismic damage model for reinforced concrete, *J Struct Eng*, 1985; **111**(4): 722–39.
13. BHRC. *Iranian code of practice for seismic resistant design of buildings, Standard, No. 2800-05*, 3<sup>rd</sup> edition, Building and Housing Research Center, Tehran, Iran, 2005.